Advances in Science and Technology Research Journal

Advances in Science and Technology Research Journal 2024, 18(4), 355–368
https://doi.org/10.12913/22998624/189464
ISSN 2299-8624, License CC-BY 4.0

Received: 2024.04.04
Accepted: 2024.06.10
Published: 2024.06.20

Study of the Effects of Heat Exchanger Location on Turbofan Engine Performance

Robert Jakubowski[1*], Arkadiusz Bednarz[1], Łukasz Rogalski[2]

[1] Department of Aerospace Engineering, Faculty of Mechanical Engineering and Aviation, University of Technology, Al. Powstańców Warszawy 8, 35-959 Rzeszów, Poland

[2] MTU Aero Engines Polska, Tajęcina 108, 36-002 Tajęcina, Poland

* Corresponding author's e-mail: robert.jakubowski@prz.edu.pl

ABSTRACT

The article presents a numerical investigation of the impact of heat exchanger (HE) location on the performance of the geared turbofan engine (GTF). It discusses the development trend for aero engines, with a primary focus on the modification of the turbofan engine cycle by the addition of the heat exchanger. This paper presents the current state of research on heat exchangers and their application in aero engines. The paper focuses on the thermodynamic model of the GTF engine, with particular emphasis on its modification to study the impact of heat exchangers on engine performance. The assumptions and limitations of the model are also discussed. The study examines the effects of various locations of the heat exchanger in the GTF engine, as well as its efficiency and pressure drop, on the engine overall performance, as measured by thrust and specific fuel consumption (SFC). The study demonstrates that the use of HE has a positive effect on engine thrust, but it also leads to an increase in SFC. According to the results, the HE should be positioned in the core engine of the GTF to achieve maximum thrust. This is achieved when the HE core flow inlet is located at approximately half the pressure ratio of the high-pressure compressor (HPC). It was found that the cold side pressure losses of the HE have a significant impact on engine performance for high bypass ratio turbofan engines. The conclusion can be drawn that when designing a heat exchanger, it is of the utmost importance to take care to minimize its impact on pressure losses in the external channel of the engine.

Keywords: turbofan engine; turbofan with heat exchanger; modified turbofan engine.

INTRODUCTION

In response to regulations from international organizations such as the European Union and the International Civil Aviation Organization, new requirements have been established for aircraft engines with the objective of limiting their detrimental impact on the environment [1]. Ongoing research is being conducted on conventionally powered aircraft with the objective of identifying issues with greenhouse gas emissions as well as other pollutants emitted during typical flight operations. These studies are based on the findings presented in works [1] and [2]. Conversely, new solutions are being developed with the aim of significantly or even completely reducing aircraft emissions, primarily through a change in propulsion system concept [3, 4]. One such option being offered to the aviation industry is electric or hybrid propulsion system [5]. Studies [5, 6] have demonstrated that using hybrid propulsion compared to conventional ones has environmental benefits.

However, due to the current state of technological advancements in the field, it is improbable that batteries or other forms of electricity will be able to efficiently power large passenger and transportation aircrafts in the near future [3, 7]. Considerable effort is constantly put into improving aircraft propulsion systems, particularly with regard to efficiency and minimizing negative environmental effects by lowering noise and

pollutant emissions [3, 7]. The goal of ongoing efforts is to alter the thermodynamic cycle and architecture of engines currently in use. One strategy to increase engine efficiency is to look for novel alternative fuels [7]. Simulation studies conducted in this area, as evidenced by works [8, 9], in conjunction with real-world experiments [10, 11], have yielded disparate results. In work [9], the potential for a significant 40% reduction in CO emissions in comparison to conventional aviation fuel has been demonstrated. Nevertheless, tests conducted on a microturbine [11] demonstrated that an increase in the content of biocomponents resulted in a discernible rise in CO emissions and a slight elevation in certain other gases (HC and NO_x).

The strategy for utilizing the current turbine engine is the modification of its cycle, which can be implemented in a number of ways. For example, adding a burner between the turbines to boost efficiency, as mentioned in [12–15]. As demonstrated in [12], the two-combustor engine exhibits a reduced total pressure ratio (smaller compressor) in order to achieve the same take-off thrust at a comparable air flow as a conventional turbofan. A diminished pressure ratio results in an elevated specific fuel consumption during take-off operations. However, during flights at high speeds, the performance of a two-combustor engine is more advantageous than that of a conventional turbofan engine. In works [13, 14], it is demonstrated that the use of an engine with an additional combustor reduces the turbine inlet temperature substantially and the associated cooling requirements and NO_x emissions.

The next promising engine modification method involves modifications to the cycle through intercooling and reheating, as discussed in [16–18]. The PW-1000 family of GTF, manufactured by Pratt and Whitney, is a highly successful type of turbofan engine modification by gear application between fan and low-pressure shaft. It has significantly reduced fuel consumption, minimized noise pollution, and increased engine efficiency [19, 20]. The concept of intercooling and regeneration as a simple jet engine modification is discussed in [16, 17, 21]. The articles cover the use of reheating and intercooling techniques to increase engine output power and thrust. Furthermore, the text discusses the use of a heat exchanger to transfer a portion of the energy from exhaust gases to the combustion chamber, which results in a reduction in fuel consumption. In reference [22], the thermodynamic cycle and technological advancements required for the implementation of an intercooler and exhaust gas recovery in a three-shaft turbofan are analyzed. The engine has been optimized for long-range flights. The weight of the heat exchanger and engine emissions has been estimated.

In [16], the performance characteristics of a traditional turbofan engine with intercooling and regeneration were examined. The analysis confirmed that the engine with only an intercooler consumes more fuel and has a lower thermal efficiency than the typical engine. On the other hand, the engine that includes both a regenerator and an intercooler has a higher thermal efficiency and uses less fuel than the typical engine. The engine that achieves the highest thermal efficiency and the lowest specific fuel consumption is the one that solely employs regeneration, even though it generates less thrust.

In [23], the authors analyze a turbofan with an intercooler application for a typical mission. The findings indicate that by increasing the overall pressure ratio (OPR) while maintaining constant combustor input and outlet temperatures, a turbofan engine without intercoolers can burn 3.4% less fuel.

Oxford University and Rolls-Royce UK conducted a study on intercooling and regeneration as part of the EU Framework 6 New Aero Engine Core Concepts (NEWAC) program [24, 25]. They designed an annular zigzag configuration around the core using corrugated heat exchangers, and the ducting system was tested by Loughborough University. Efforts were made to minimize the installation penalty of the intercooler system [26, 27] and reduce pressure loss in both the intercooler and its ducting system [28, 29]. In order to optimize the bend of the intercooled core, it is important to reduce pressure loss and minimize installation penalties. The study of pressure loss investigation in the heat exchanger intended for aero engines is presented in [30, 31]. A heat exchanger made of elliptic cross-section U-tubes stacked in a 4/3/4 pattern is tested in this work. The study verifies that the sort of heat exchanger under examination may be fitted using a quite straightforward quadratic pressure drop rule. It is also stated that the modeling approach described here cannot be applied to any random form of heat exchanger used in an aero engine.

The intent of work done in [32] was to optimize heat exchanger shapes for the recuperation process. Two entirely new and cutting-edge heat exchanger concepts were produced as a result of the geometry

optimization procedure that was supplied through CFD computing to maximize the recuperation benefits of the intercooled recuperated aero engine. The findings demonstrate that it is feasible to lower specific fuel consumption (SFC) by more than 10% by adhering to the heat exchanger approach.

A 3D printed shell-and-tube heat exchanger featuring an octahedral lattice structure was the subject of a recent study presented in [33]. An inquiry into experiments was conducted to validate the study's simplified description of the heat-flow process. The outcomes demonstrated that as flow rate increases on the tube side, so does the effectiveness of heat transmission. Under the heat exchanger's tested conditions, the tested facility's heat transfer effectiveness ranges from 0.7 to nearly 0.85.

The utilization of heat exchangers in commercial turbofan engines remains an unsolved topic. No commercial engine has been put yet into operation, but research in this field is underway. The two heat exchanger positions in the core engine, one for recuperation after the high-pressure compressor (HPC) and one for reheating between the low-pressure compressor (LPC) and HPC, have been the subject of research on aero engines. While there have been suggestions for specific remedies for heat exchanger (HE) in various areas, HE localization within the HPC have not been investigated yet. The compressor with heat exchanger requires redesigning, and its axial size must be increased for HE inlet and outlet location. However, the development of such an engine concept could be pursued if this redesign improves the engine's performance. This paper models and analyzes the impact of the several positions of the heat exchanger within the HPC on engine performance.

TURBOFAN ENGINE CONCEPT WITH HEAT EXCHANGER AND ITS NUMERICAL MODEL

The GTF engine was selected to investigate the influence of the HE location on engine performance. Previous studies have shown that the GTF has a more favorable pressure distribution between compressors due to its higher low-pressure compressor pressure ratio (LPC PR) compared to the classical turbofan (TF) [19, 20]. As a result, the gas temperature in the LPC outlet is higher, making the heat exchanger located after the LPC more efficient. This study assumes a counter-flow heat exchanger due to its higher efficiency in heat exchange [34]. Previous works have studied this type of heat exchanger [16–18]. The study examines a GTF engine with a heat exchanger, but the presented results can be generalized to other types of turbofan engines.

Figure 1 presents the cross-section numbering of the tested engine schemes. The base engine (Fig. 1a) is the GTF without HE. GTF with HE located before HPC called HE (1) is shown in Figure 1b. GTF with HE located in the middle of HPC – HE (2) is on Figure 1c and the GTF with HE in the exit of HPC – HE (3) is in Figure 1d. The cross-section specification of the engine presented in Figure 1 is used in the engine model and analysis. The nomenclature of the main cross-sections applied is typical for a bypass engine and therefore will not be discussed in detail. However, additional HE cross-sections are briefly presented. Section 26 is located in the HE inlet of the core engine, and section 28 is located in the HE outlet of the core engine. In certain locations of the heat exchanger, such as between the LPC and HPC in the core engine, section 26 is identical to section 23 (LPC outlet), and section 28 is identical to section 25 (HPC inlet). In the bypass flow heat exchanger, the inlet is labeled 13 and the outlet is labeled 16, as shown in Figure 2. In section 26, the temperature of the core flow entering the HE is higher than the temperature of the bypass flow in section 13. As a result, the temperature of the bypass flow (cold side flow) increases in the HE, while the temperature of the core flow (hot side flow) decreases. According to [34], for steady-state analysis where heat accumulation in the HE material can be neglected, the energy balance is written as:

$$\dot{Q}_{Ex} = \dot{m}_{13} cp_1 (T_{t16} - T_{t13}) = \\ = \dot{m}_{26} cp_2 (T_{t26} - T_{t28}) \quad (1)$$

where: $\dot{Q}_{Ex}$ [J/s] – heat flow rate through a heat exchanger, $\dot{m}_{13}$ [kg/s] – heat exchanger cold side air mass flow rate, $\dot{m}_{26}$ [kg/s] – heat exchanger hot side air mass flow rate, cp_1 and cp_2 [J/(kg·K)] – the specific heat values at constant pressure of air in the temperature range (T_{t16}-T_{t13}) and (T_{t26}-T_{t28}) respectively, T_t [K] – total temperature of gas in the specified engine section.

To evaluate exchanger heat flow rate, its efficiency is defined as [34]:

$$\eta_{Ex} = \frac{\dot{Q}_{Ex}}{\dot{Q}_{Ex\_max}} \quad (2)$$

where: $\dot{Q}_{Ex}$max is the maximum possible heat flow rate. In counter-flow heat exchanger, the maximum possible heat exchange is defined as the smaller value of:

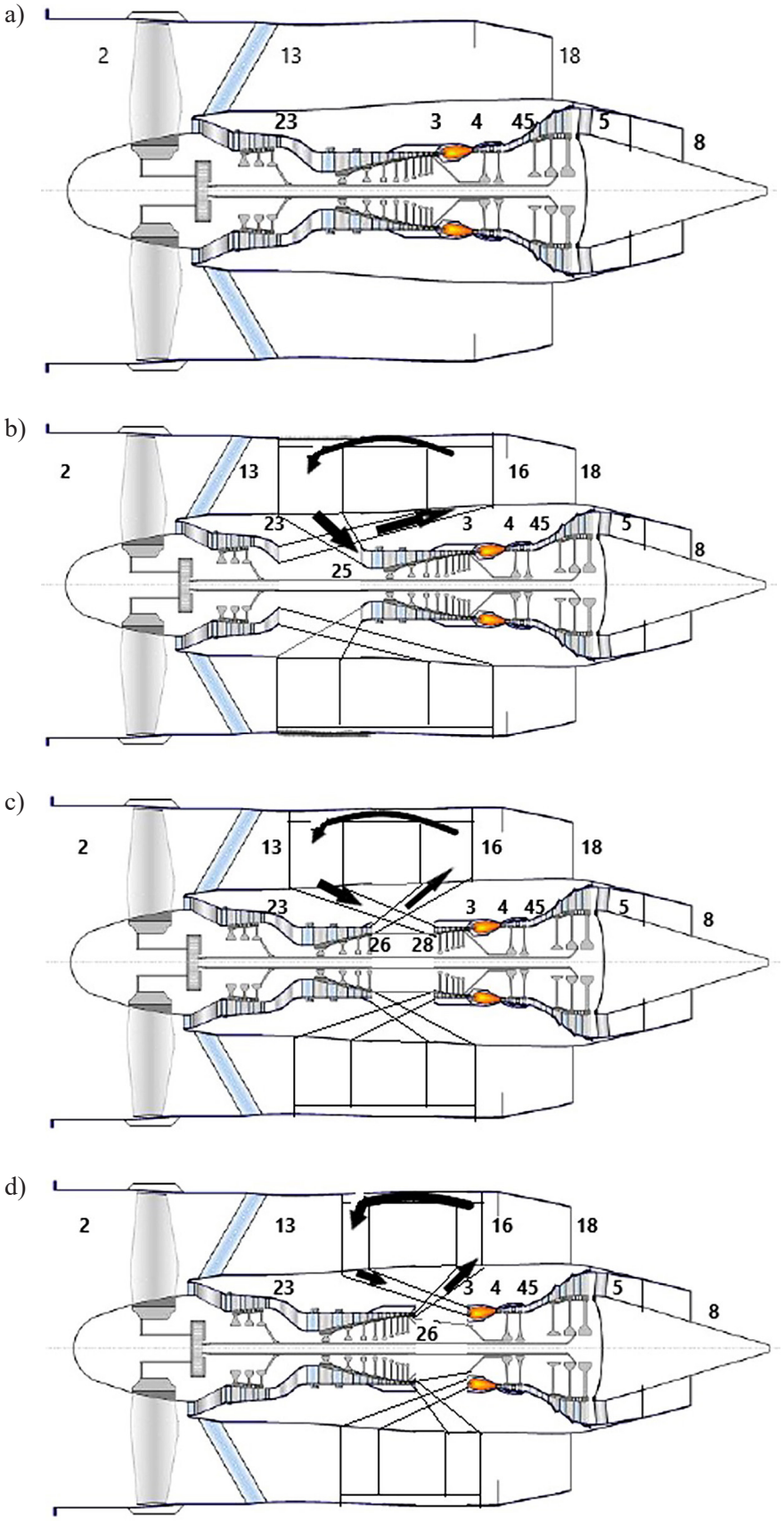

Figure 1. Cross section of a) GTF, b) GTF with heat exchanger between LPC and HPC – HE (1), c) GTF with heat exchanger in HPC – HE (2), and d) GTF with heat exchanger after HPC – HE (3)

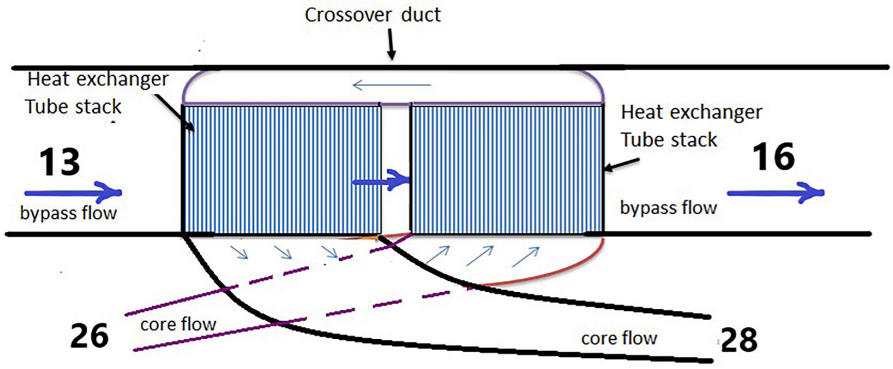

Figure 2. Heat exchanger cross section.

$$\dot{Q}_{Ex\_max} = \min \begin{cases} \dot{m}_{13} cp_1 (T_{t26} - T_{t13}) \\ \dot{m}_{26} cp_2 (T_{t26} - T_{t13}) \end{cases} \quad (3)$$

For a high bypass ratio (BPR) engine, the core flow rate ($\dot{m}_{26}$) is significantly lower than the bypass flow rate ($\dot{m}_{13}$). Additionally, the heat values at constant pressure are at a similar level for both streams. Therefore, minimum heat flow rate is:

$$\dot{Q}_{Ex\_max} = \dot{m}_{23} cp_1 (T_{t26} - T_{t13}) \quad (4)$$

The pressure loss on the hot and cold side of the heat exchanger is an important feature of HE. Pressure loss modelling and evaluation for different types of heat exchangers have been examined in various studies [23, 26, 29–31, 33]. The results indicate that pressure loss follows HE construction and flow parameters, such as mass flow rate, flow velocity, and Reynolds number. According to the results in [33], hot side pressure losses are significantly higher than cold side losses. The hot side tube is thinner and has a more complex flow channel, which increases flow resistance. In contrast, the cold side has lower flow resistance due to its aligned tube arrangement. The results indicate that pressure losses range from 14-26% for the hot side flow and about 1% for the cold side in the tested HE type.

This work presents a methodology for calculating pressure losses in a heat exchanger, utilizing coefficients for the hot and cold sides, defined as follows:

$$\sigma_{Ex\_h} = \frac{P_{t28}}{P_{t26}} \quad (5)$$

$$\sigma_{Ex\_c} = \frac{P_{t16}}{P_{t13}} \quad (6)$$

where: P_t [Pa] represents the total pressure of the gas flow in the heat exchanger sections as specified by the subscript.

This study assumes a general counter-flow HE, rather than any previously tested specified type. The purpose of this study is to investigate the location of the HE and its influence on the bypass engine performance. Detailed construction of the HE is not a goal of this work, therefore the engine mass growth due to HE application is not analyzed. The authors are aware that HE application increases engine mass and length, but a more detailed engine definition is needed for analysis in this case. The GTF thermodynamic model was used in this study to analyze the overall impact of HE on engine performance. The examined HE efficiency ranged from 50% to 90%, with cold side pressure losses of 3% and hot side losses of 8%. When examining HE pressure losses, HE efficiency of 70% was assumed.

The MATLAB preparation of the GTF engine and the GTF with heat exchanger engine model employs the 1D mean line model, which considers the secondary air flow for turbine cooling as presented in [19, 36]. Figure 3 illustrates the functional blocks model for the GTF with heat exchanger between LPC and HPC. For other HE locations engine model is similar with the HE offset along the HPC.

The functional blocks represent the numerical model of the engine components, including the inlet, fan, compressor, burner, turbine, propelling nozzle, and heat exchanger. These blocks cover the typical equations describing energy, mass, and momentum conversion found in literature (e.g., [21, 37]). The semi-perfect gas model presented

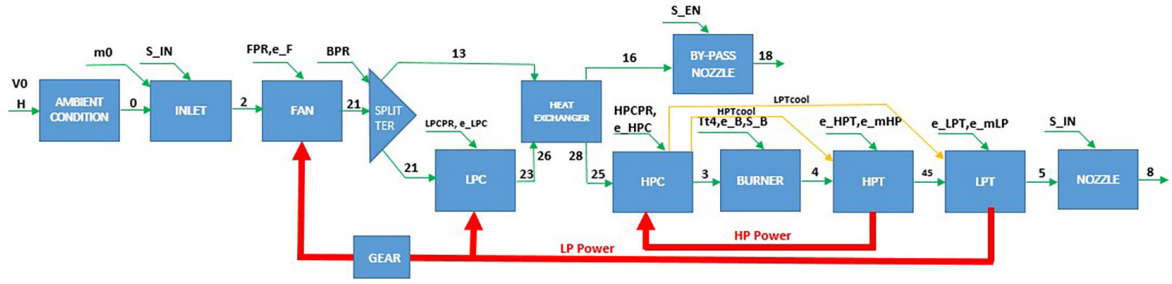

Figure 3. Functional block model of the GTF with a heat exchanger

in work [38] is applied to the GTF engine internal flow modeling. Flow parameters, such as gas mass flow, temperature, and pressure, are transferred among the blocks. The HPC, HPT, Fan, LPC, and LPT are matched by energy balance. The bleeds in the engine compressor section for turbine cooling and customer purposes are modeled according to references [21, 37]. The cooling turbine model is adopted from reference [39]. Flow continuity equations are fulfilled inside the engine. Additional parameters, such as pressure loss and efficiencies of some engine components, are specified according to contemporary high bypass GTF engine data presented in references [17, 36].

The analysis presents the design point (DP) which is defined by an altitude of 11 km, a flight Mach number of 0.8, an air mass flow of 240 kg/s, and ambient pressure and temperature specified by The International Standard Atmosphere (ISA). Table 1 shows the other main engine parameters. In the engine analysis with HE, all parameters such as the HPT turbine inlet temperature (TIT) and overall pressure ratio (OPR) and efficiencies of the engine components are at the same level as for the base GTF. Heat exchangers introduce additional pressure and thermal losses, which are discussed below. In all cases where the engine is equipped with HE, the outlet temperature of the HPC is expected to be lower than that of the base engine. The HPT cooling bleed is located in this area. To compensate for the lower coolant temperature in the HPT cooling process, the coolant mass flow is reduced.

For the base GTF without HE, it is assumed that there is HPC bleed after the 4-th stage of 3% core flow for LPT cooling and additional bleed after HPC of 8% core flow for HPT cooling. For the GTF with HE, it is assumed that the air bleed for HPT cooling is located in the same position as in the base GTF. The amount of extracted coolant decreases to provide the same amount of heat extracted from the main stream of HPT as in the base GTF. This Equation is satisfied for all studied engines:

$$\dot{Q}_{HPT\_cool} = \dot{m}_{23}\,\beta_{cool}\,cp\,(T_{t4} - T_{t3}) = const \quad (7)$$

where: $\dot{Q}_{(HPT\_cool)}$ [J/s] – heat exchanged between the cooling flow and the HPT main flow, $\dot{m}_{26}$ [kg/s] –engine core mass flow rate, β_{cool} [-] – HPT coolant mass flow to core engine mass flow ratio, T_{t3}, T_{t4} [K] – total temperatures at engine sections 3 (HPC outlet) and 4 (HPT inlet). For GTF with a heat exchanger, β_{cool} decreases due to a decrease in HPC outlet temperature T_{t3}.

The objective of this study is to analyze the engine thrust and SFC of the studied engines. The net thrust of the turbofan engine and is defined as follows:

$$T = \dot{m}_8 u_8 + A_8(P_8 - P_a) + \\ + \dot{m}_{18} u_{18} + A_{18}(P_{18} - P_a) - \dot{m}_2 u_0 \quad (8)$$

Specific fuel consumption is defined as:

$$SFC = \frac{\dot{m}_{fuel}}{T} \quad (9)$$

Table 1. GTF engine main parameters

Parameter	Symbol	Unit	Value
Bypass ratio	BPR	–	12
Fan pressure ratio	FPR	–	1.42
Low pressure compressor pressure ratio	LPC PR	–	2.3
High-pressure compressor pressure ratio	HPC PR	–	13.9
Turbine inlet temperature	TIT	K	1680

where: T [N] – net thrust, SFC [kg/(N·s)] – specific fuel consumption, $\dot{m}_2$, $\dot{m}_8$, m_{18}, [kg/s] – mass flow rate at the engine inlet, internal nozzle exit and external nozzle exit, $\dot{m}_{fuel}$ [kg/s] – fuel mass flow rate u_0, u_8, u_{18}, [m/s] – flight speed, flow velocity at the internal nozzle exit and at the external nozzle exit, P_a [Pa] – static ambient pressure, P_8, P_{18} [Pa] – static pressure at the internal and external nozzle exit, A_8, A_{18} [m^2] – area of internal and external nozzle exit.

RESULTS AND DISCUSSION

The impact of various HE locations for various efficiencies on GTF engine performance is presented in relation to the base GTF engine. Therefore, Table 2 shows the data calculated for the GTF without HE. The main performance parameters are similar to the data presented in [20], where the PW1100 engine is analyzed.

Impact of heat exchanger efficiency and its location on engine performance

Table 3 presents the results of engine performance parameter calculations for three specified locations of the HE in comparison with the GTF without HE. The third column contains the results for the GTF without HE, the fourth one for the HE located between LPC and HPC, the fifth one for the HE located inside HPC, and the last one for the HE located after HPC. The presented results are for 70% HE efficiency. It appears that the engine thrust increases with the application of HE, with the greatest thrust being for the GTF with HE located inside HPC.

The use of HE application has a negative impact on fuel-consumption, as it causes a rise in fuel mass flow that is not compensated by an increase in thrust. This results in an observed rise in SFC. The significant increase in fuel consumption is caused by a decrease in burner inlet temperature Tt31 in GTF with HE, which is more prominent when the HE is located further inside the HPC.

Figure 4 presents the results for a wide range of HE efficiency, from 50% to 90%. Relative thrust is calculated by dividing the thrust by the base GTF, and relative SFC is calculated by dividing the SFC by the base GTF SFC.

The optimal improvement in thrust is achieved when the entrance to the HE from the internal duct is positioned inside the HPC, as shown for HE(2) in Figure 4a. A slightly lower increase in thrust is achieved when the HE is located behind the HPC, as shown for HE(3). Placing the HE between the LPC and HPC results in only a slight increase in thrust (HE(3)). In all cases studied, an increase in HE efficiency positively influenced engine thrust.

It was found that the SFC increases in all cases of HE locations (Fig. 4b), which is a negative effect of HE application. This phenomenon has also been observed in recent studies [17,

Table 2. Calculated GTF engine at design point

Parameter	Unit	Value
Inlet air mass flow	kg/s	240
Core engine mass flow	kg/s	18.46
Fuel mass flow	kg/h	1484
Thrust	kN	25.78
Specific fuel consumption	kg/N/h	0.057565

Table 3. Chosen performance parameters for the GTF without HE and the GTF with HE located at three locations in the HPC.

Parameter	Unit	No HE	HE (1)	HE (2)	HE (3)
HE efficency	%	-	70	70	70
T_{t31}	K	811	682	539	435
B_HPTcool	-	0.08	0.0696	0.0609	0.0541
Fuel mass flow	kg/h	1484	1725	1992	2189
Thrust	kN	25.78	26.90	28.66	28.43
SFC	kg/N/h	0.057565	0.064138	0.069488	0.076995

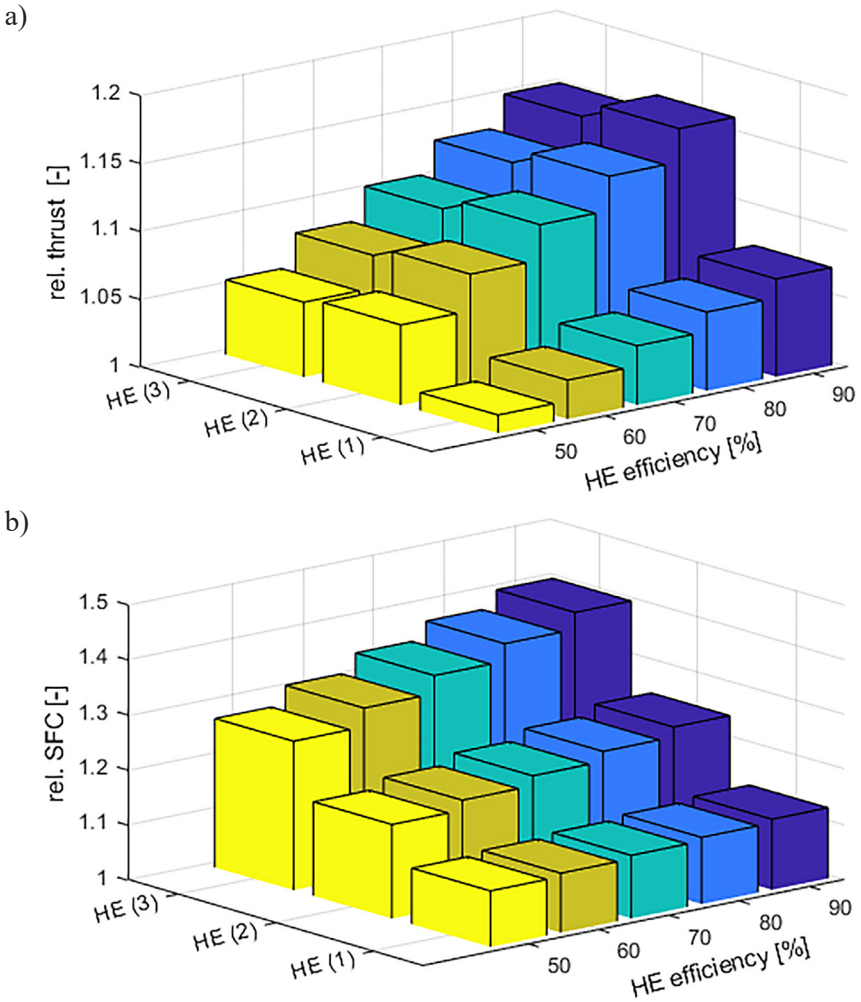

Figure 4. a) relative thrust of GTF with a heat exchanger, b) relative SFC of GTF with a heat exchanger

18, 21], in which the heat exchanger was situated between the low-pressure and high-pressure compressors. The results demonstrate that the location of HE has a significant impact on SFC. However, if HE is located more towards the front of the engine, the increase in SFC is smaller. When HE is located closer to the burner in the core engine, there is a significant increase in SFC. The efficiency of HE has a smaller impact on SFC, particularly for HE located at the front of the engine. When the HE is located closer to the combustion chamber, its efficiency has a greater effect, resulting in a higher increase in SFC. In general, it can be concluded that an increase in HE efficiency has a positive impact on thrust and a negative impact on SFC.

The results presented suggest that the location of the HE relative to the HPC has a significant impact on engine performance, particularly on thrust growth. Therefore, it is possible to optimize thrust by specifying the HE location in the core engine. Simulations were conducted to test this hypothesis, with HE efficiencies of 70% and 80%, while varying the position of the HE location in the HPC. The results are presented in Figure 5, where HE PR in HPC corresponds to the HPC PR. In the case where HE PR in HPC = 1, this indicates that HE is before HPC, while HE PR in HPC = 14 signifies that HE is behind HPC. All other intermediate values correspond to the heat exchanger location at a specific value of the HPC PR. The results indicate that the maximum thrust is achieved when the HE is located in HPC PR about 6–7, which is approximately half of HPC PR, regardless of the HE efficiency. Higher HE efficiency leads to a higher thrust increase, which is consistent with previously presented results.

SFC continuously increases as the HE location is moved along the HPC. Higher HE efficiency enhances the effect of SFC growth.

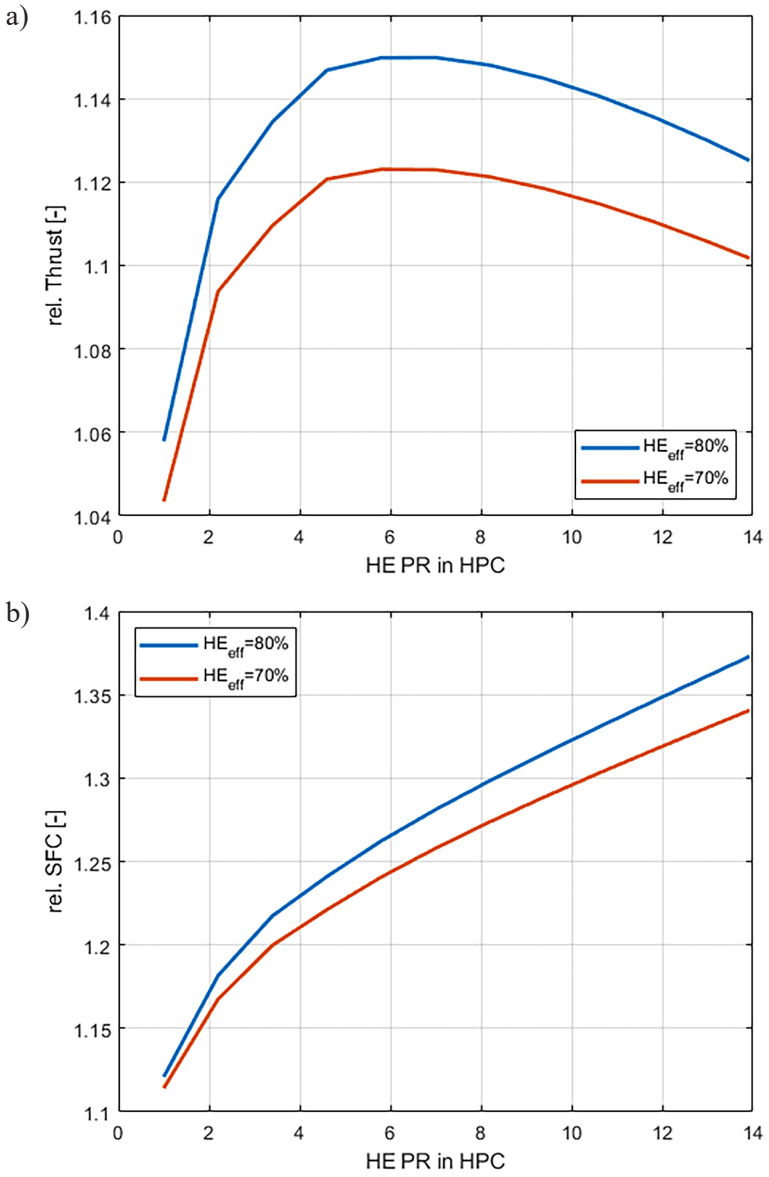

Figure 5. Results of HE location measured by HE PR for two HE efficiencies a) relative thrust, b) relative SFC

Impact of heat exchanger pressure losses and its location on engine performance

This chapter discusses the impact of pressure losses in the HE on engine performance. The initial pressure loss was assumed to be 3% for the cold side and 8% for the hot side of the HE. Figure 6 shows the results for this case represented by the blue line. The other presented lines are for decreased pressure losses of one HE side of 10% and 20% respectively. Thus for HE cold side pressure losses reduction of 10% and 20% pressure losses coefficient is 0.986 and 0.984 while HE hot side loss coefficient is kept constant and equal to 0.92. (lines purple and green).For HE hot side pressure losses reduction of 10% and 20% pressure losses coefficient is 0.928 and 0.836 while HE cold side pressure loss coefficient is kept constant and equal to 0.97 (lines red and orange).

The results demonstrate that reducing pressure losses in the HE has a positive effect on engine performance, resulting in increased thrust (as shown by the blue line at the bottom of Figure 6a) and decreased SFC (as shown by the blue line at the top of Figure 6b). Notably, reducing pressure losses on the cold side of the HE has a greater impact on the analyzed parameters than reducing losses on the hot side. Specifically, a 10% reduction in cold side pressure losses yields better results than a 20% reduction in hot side losses. The higher bypass

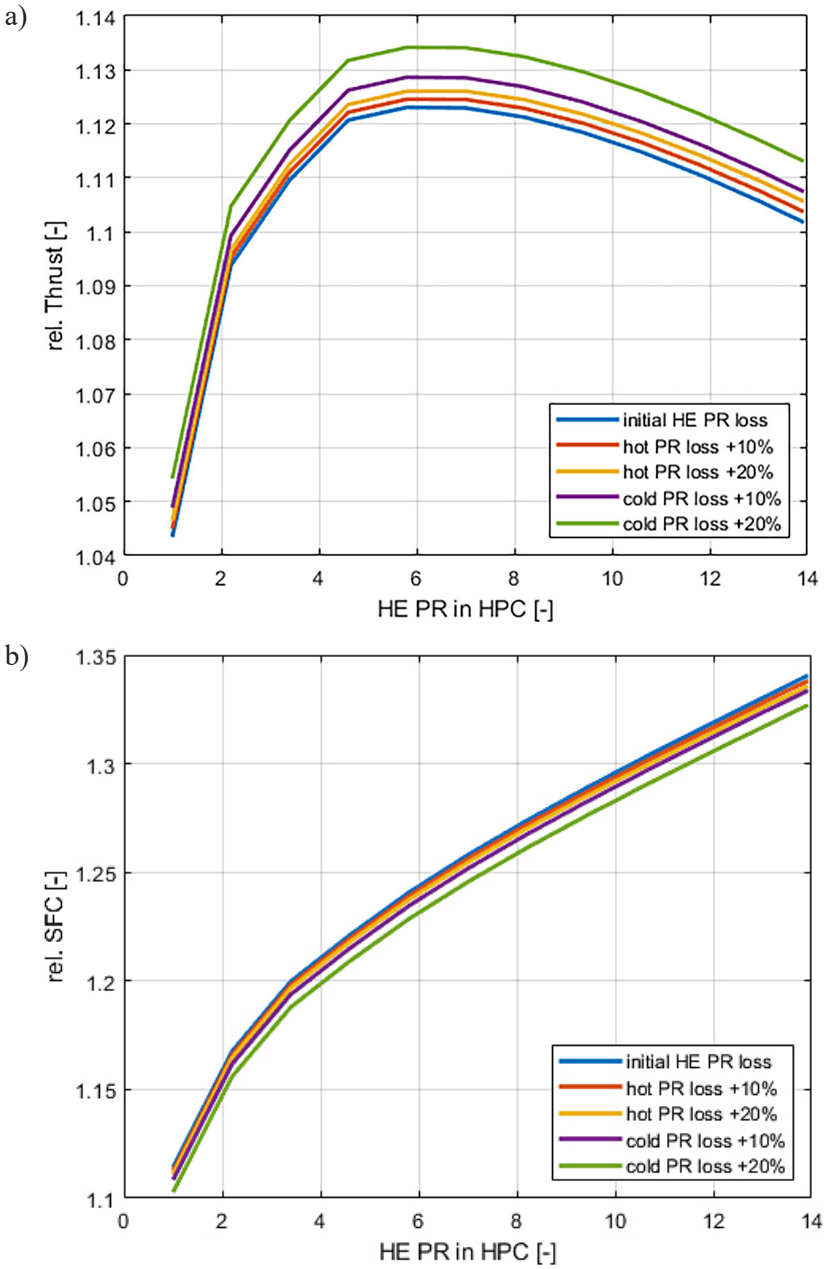

Figure 6. Results of HE location measured by HE PR at HPC for initial HE pressure loss and pressure losses improved by 10% and 20% a) relative thrust, b) relative SFC

ratio (BPR) of the analyzed engine results in a greater effectiveness of pressure loss reduction on the cold side. This is due to the larger airflow in the bypass engine and its contribution to engine thrust production.

To provide a more comprehensive illustration of the outcomes depicted in Figure 6, Figure 7 presents the results for HE situated at HPC PR = 7, which yielded the most pronounced thrust enhancement. ΔT and ΔSFC are defined as:

$$\Delta T = \frac{T(red\ PR\ loss) - T(initial\ PR\ loss)}{T(initial\ PR\ loss)} \times 100\% \quad (10)$$

$$\Delta SFC = \frac{SFC(red\ PR\ loss) - SFC(initial\ PR\ loss)}{SFC(initial\ PR\ loss)} \times 100\% \quad (11)$$

where: *red PR loss* means reduced pressure loss of HE, and *initial PR loss* means pressure losses initially assumed: 3% for the cold side and 8% for the hot side of HE.

Reducing pressure losses has a similar impact on both engine thrust and SFC. Specifically, a 10% reduction in hot side HE PR loss results in a 0.2% increase in thrust and a corresponding decrease in SFC. Similarly, a 20% reduction in cold side HE pressure losses leads to a 1% increase in

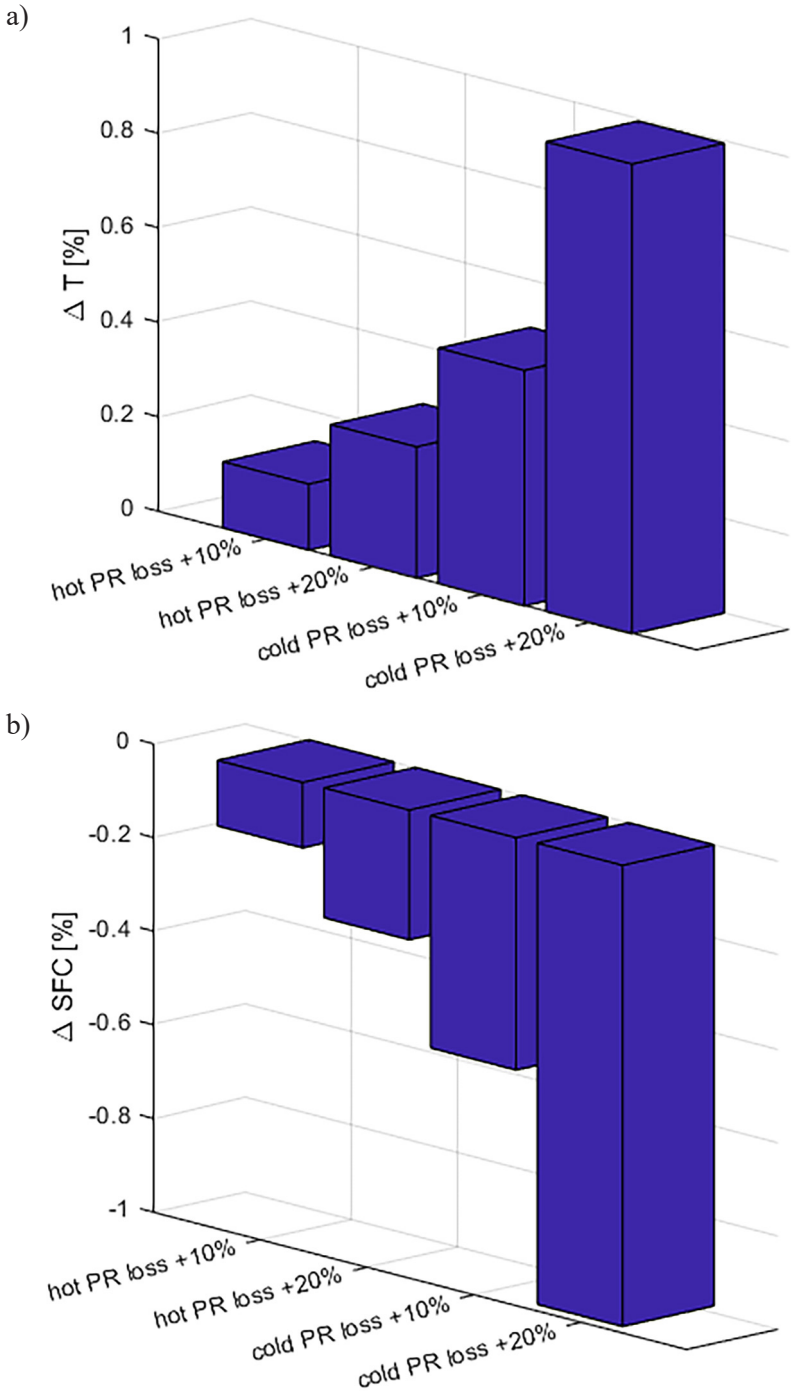

Figure 7. a) Engine thrust increase and b) SFC decrease by HE pressure losses reduction

thrust and a corresponding 1% decrease in SFC. In general, reducing HE pressure losses has a positive impact on engine performance. For the tested high bypass ratio GTF, reducing pressure losses in the cold HE side has a stronger effect than reducing pressure losses in the hot side HE. This suggests that in GTF HE design, particular attention should be paid to reducing pressure losses in the cold side (bypass duct flow). However, achieving this requires a compromise between HE efficiency and pressure losses, as increasing HE efficiency would necessitate a more complex HE design, resulting in a higher pressure drop [34].

CONCLUSIONS

The geared turbofan engine with a heat exchanger is a prospective solution for improving the efficiency of large turbofan engines that

power passenger and transport aircraft. Research in this area focuses on developing the heat exchanger and analyzing the engine's performance with it. Previous studies have tested engines with HE mounted between the low- and high-pressure compressors. This study examines the effect of HE located inside the HPC on engine performance.

The main conclusion of the work is that placing the HE inside the HPC allows for a larger growth in engine thrust compared to when the HE is placed before or behind the HPC. In the analyzed cases, the forecasted increase in thrust is up to 18% compared to the base engine without HE. A detailed analysis of the location of the HE along the HPC reveals that the greatest thrust is achieved when the HE is positioned inside the HPC, with the PR at approximately 0.5 times the HPC PR. This suggests that the concept of placing the HE inside the HPC has great potential for increasing thrust.

The use of HE in the GTF leads to an increase in fuel consumption and additionally SFC grow. This effect is not favorable, as the increase in fuel consumption significantly exceeds the increase in thrust.

Furthermore, increasing HE efficiency has a positive impact on thrust but causes an unexpected increase in SFC. A positive effect is observed when reducing HE pressure losses. This results in increased thrust and reduced SFC. These effects are more significant for HE cold side pressure drop reduction.

However, this study only assesses the impact of HE application on the engine's performance, without considering other factors such as the increased weight and length of the engine or the analysis of heat exchanger construction to meet the strength requirements resulting from the increased pressure difference between the core flow and bypass flow. These aspects will be subjected to further investigation in future studies once the engine in question has been accepted for use with the HE concept. Our efforts will continue to focus primarily on seeking modifications to the engine with a HE that will result in a reduction in SFC. We expect to achieve this by, for example, increasing the engine pressure ratio while considering all limitations, including the minimum blade height as in [40]. The next significant issue to consider will be the impact of this solution on the change in engine rotors dynamics and the resulting loads generated on the engine bearings. The alteration of rotor dimensions and the positioning of supports can present a significant challenge, particularly in the context of operational loads on turbine engines, as evidenced by the findings in [41, 42].

REFERENCES

1. Markowski, J., Pielecha, J. Selected issues in exhaust emissions from aviation engines. J. Merkisz (Ed.). Nova Science Publishers, Incorporated, 2014.
2. Pawlak, M., Kuźniar, M. Determination of CO_2 emissions for selected flight parameters of a business jet aircraft. Journal of KONES, 2019; 26(3): 155–163. https://doi.org/10.2478/kones-2019-0069
3. Lei, T., Min, Z., Gao, Q., Song, L., Zhang, X., Zhang, X. The Architecture Optimization and Energy Management Technology of Aircraft Power Systems: A Review and Future Trends. Energies 2022; 15(11): 4109. https://doi.org/10.3390/en15114109
4. Orkisz, M., Kuźniar, M. 3E-A new paradigm for the development of civil aviation. Combustion Engines 2020; 181(2): 3–10. https://doi.org/10.19206/CE-2020-201
5. Pawlak, M., Kuźniar, M. Performance and Emission of the Aircraft with Hybrid Propulsion During Take-Off Operation Cycle. Advances in Science and Technology Research Journal 2024; 18(1): 155–166. https://doi.org/10.12913/22998624/177254
6. Kuźniar, M., Pawlak, M., Orkisz, M. Comparison of Pollutants Emission for Hybrid Aircraft with Traditional and Multi-Propeller Distributed Propulsion. Sustainability 2022; 14(22): 15076. https://doi.org/10.3390/su14116488
7. Reitz, R.D., Ogawa, H., Payri, R., Fansler, T., Kokjohn, S., Moriyoshi, Y., Zhao, H. The future of the internal combustion engine. International Journal of Engine Research 2020; 21(1): 3–10. https://doi.org/10.1177/1468087419877990
8. Wasiak, A., Orynycz, O., Tucki, K., Świć, A. Hydrogen enriched hydrocarbons as new energy resources–as studied by means of computer simulations. Advances in Science and Technology Research Journal 2022; 16(5): 78–85. https://doi.org/10.12913/22998624/154001
9. Pawlak, M., Kuźniar, M. The Effects of the Use of Algae and Jatropha Biofuels on Aircraft Engine Exhaust Emissions in Cruise Phase. Sustainability 2022; 14(11): 6488. https://doi.org/10.3390/su14116488
10. Seyam, S., Dincer, I., Agelin-Chaab, M. Novel hybrid aircraft propulsion systems using hydrogen, methane, methanol, eth-anol and dimethyl ether as alternative fuels. Energy Conversion and Management 2021; 238: 114172. https://doi.org/10.1016/j.enconman.2021.114172
11. Przysowa, R., Gawron, B., Białecki, T., Łęgowik,

A., Merkisz, J., Jasiński, R. Performance and emissions of a microturbine and turbofan powered by alternative fuels. Aerospace 2021; 8(2): 25. https://doi.org/10.3390/aerospace8020025

12. Jakubowski, R. Evaluation of performance properties of two combustor turbofan engine. Eksploatacja i Niezawodnosc – Maintenance and Reliability 2015; 17(4): 575–581. https://doi.org/10.1016/j.ast.2018.03.005
13. Yin, F., Rao, A.G. A review of gas turbine engine with inter-stage turbine burner. Progress in Aerospace Sciences 2020; 121: 100695, https://doi.org/10.1016/j.paerosci.2020.100695
14. Yin, F., Rao, A.G. Performance analysis of an aero engine with inter-stage turbine burner. The Aeronautical Journal 2017; 121(1245): 1605–1626. https://doi.org/10.1017/aer.2017.93
15. Yin, F., Rao, A.G. A review of gas turbine engine with inter-stage turbine burner. Progress in Aerospace Sciences 2020; 121: 100695. https://doi.org/10.1016/j.paerosci.2020.100695
16. Lebre, J., Brójo, F. Performance of a Turbofan Engine with Intercooling and Regeneration. International Journal of Aero-space and Mechanical Engineering 2011; 5(6): 1034–1038.
17. Andriani, R., Gamma, F., Ghezzi, U. Regeneration and Inter-cooling in Gas Turbine Engines for Propulsion Systems. In 44th AIAA/ASME/SAE/ASEE Joint Propulsion Conference Exhibit 2008; 4899. https://doi.org/10.2514/6.2008-4899
18. Wilfert, G., Kriegl, B., Scheugenpflug, H., Bernard, J., Ruiz, X., Eury, S. Clean-Validation of a High Efficient Low NOx Core, a GTF High Speed Turbine and an Integration of a Re-cuperator in an Enviromental Friendly Engine Concept. In 41st AIAA/ASME/SAE/ASEE Joint Propulsion Conference Exhibit 2005; 4195. https://doi.org/10.2514/6.2005-4195
19. Kurzke, J. Fundamental differences between conventional and geared turbofans. In Turbo Expo: Power for Land, Sea, and Air 2019; 48821: 145–153. https://doi.org/10.1115/GT2009-59745
20. Sato, A., Imamura, M., Fujimura, T. Development of pw1100g-jm turbofan engine. IHI Engineering Review 2014; 47(1): 23–28.
21. Kurzke, J., Halliwell, I. Propulsion and power: an exploration of gas turbine performance modeling. Cham, Switzerland: Springer international publishing 2018; 355. https://doi.org/10.1007/978-3-319-75979-1
22. Boggia, S., Rüd, K. Intercooled recuperated gas turbine engine concept. In 41st AIAA/ASME/SAE/ASEE Joint Pro-pulsion Conference Exhibit 2005; 4192. https://doi.org/10.2514/6.2005-4192
23. Xu, L., Grönstedt, T. Design and analysis of an intercooled turbofan engine. Journal of Engineering for Gas Turbines and Power 2010; 132(11). https://doi.org/10.1115/1.4000857
24. Rolt, A.M., Kyprianidis, K. Assessment of new aero engine core concepts and technologies. in the EU framework 6 NEWAC programme. In ICAS 2010 Congress Proceedings 2010; 408.
25. Rolt, A., Baker, N.J., and Rolls-Royce plc. Intercooled Tur-bofan Engine Design and Technology Research. in the EU Framework 6 NEWAC Programme 2009.
26. A'Barrow, C., Carrotte, J.F., Walker, A.D., Rolt, A.M. Aerodynamic performance of a coolant flow off-take down-stream of an OGV. In Turbo Expo: Power for Land, Sea, and Air 2011; 54679: 187–199. https://doi.org/10.1115/GT2011-45888
27. Kwan, P.W., Gillespie, D.R., Stieger, R.D., Rolt, A.M. Minimising loss in a heat exchanger installation for an intercooled turbofan engine. In Turbo Expo: Power for Land, Sea, and Air 2011; 54617: 189–200. https://doi.org/10.1115/GT2011-45814
28. Walker, A.D., Carrotte, J.F., Rolt, A.M. Duct aerodynamics for intercooled aero gas turbines: constraints, concepts and design methodology. In Turbo Expo: Power for Land, Sea, and Air 2009; 48883: 749–758. https://doi.org/10.1115/GT2009-59612
29. Walker, A.D., Regunath, G.S., Carrotte, J.F., Denman, P.A. Intercooled aero-gas-turbine duct aerodynamics: Core air delivery ducts. Journal of Propulsion and Power 2012; 28(6): 1188–1200. https://doi.org/10.2514/1.B34450
30. Missirlis, D., Yakinthos, K., Palikaras, A., Katheder, K., Goulas, A. Experimental and numerical investigation of the flow field through a heat exchanger for aero-engine applications. International Journal of Heat and Fluid Flow 2005; 26(3): 440–458. https://doi.org/10.1016/j.ijheatfluidflow.2004.10.003
31. Missirlis, D., Yakinthos, K., Storm, P., Goulas, A. modeling pressure drop of inclined flow through a heat exchanger for aero-engine applications. Int. J. Heat Fluid Flow 2007; 28: 512–515. https://doi.org/10.1016/j.ijheatfluidflow.2006.06.005
32. Misirlis, D., Vlahostergios, Z., Flouros, M., Salpingidou, C., Donnerhack, S., Goulas, A., Yakinthos, K. Optimization of heat exchangers for intercooled recuperated aero engines. Aerospace 2017; 4(1), 14. https://doi.org/10.3390/aerospace4010014
33. Zhao, B., Zhang, J., Lian, W. Numerical modeling of heat exchanger filled with octahedral lattice frame porous material. Aerospace 2022; 9(5): 238. https://doi.org/10.3390/aerospace9050238
34. Zohuri, B. Compact heat exchangers. Cham, Switzerland: Springer. 2022 https://doi.org/10.1007/978-3-319-29835-1
35. Li, H., Huang, H., Xu, G., Wen, J., Wu, H. Performance analysis of a novel compact air-air heat exchanger for aircraft gas turbine engine using LMTD method. Applied thermal engineering

2017; 116: 445–455. http://dx.doi.org/10.1016/j.applthermaleng.2017.01.003

36. Ng, H.S. Advanced Gas Turbine Concepts: Turbofan with Intercooling and Regeneration, Turbofan with Intercooling and Regenerat - Warning: TT: undefined function: 32 Han Shing Ng 2229791 - Studocu
37. Jakubowski, R. Modelowanie osiągów silników turbinowych w środowisku MATLAB z wykorzystaniem modeli bloków funkcjonalnych. TTS Technika Transportu Szynowego 2015; 12: 691–696.
38. Guha, A. An efficient generic method for calculating the properties of combustion products. Proceedings of the Institution of Mechanical Engineers, Part A: Journal of Power and Energy 2001; 215(3): 375–387. https://doi.org/10.1243/0957650011538596
39. Masci, R., Sciubba, E. A gas turbine cooled-stage expansion model for the simulation of blade cooling effects on cycle performance. International Journal of Turbomachinery, Propulsion and Power 2019; 4(4): 36. https://doi.org/10.3390/ijtpp4040036
40. Gronstedt, T. and Kyprianidis, K. Optimizing the Operation of the Intercooled Turbofan Engine. In ASME Turbo Expo 2010. https://doi.org/10.1115/GT2010-22519
41. Wendeker, M., Czyż Z. Analysis of the bearing nodes loads of turbine engine at an unmanned helicopter during a jump up and jump down maneuver. Eksploatacja i Niezawodnosc – Maintenance and Reliability 2016; 18(1): 89–97. http://dx.doi.org/10.17531/ein.2016.1.12
42. Czyż, Z., Magryta, P. Analysis of the operating load of foil-air bearings in the gas generator of the turbine engine during the acceleration and deceleration maneuver. Eksploatacja i Niezawodnosc – Maintenance and Reliability 2016; 18(4): 507–513. http://dx.doi.org/10.17531/ein.2016.4.5